BULLETIN OF THE POLISH ACADEMY OF SCIENCES
TECHNICAL SCIENCES, Vol. 61, No. 2, 2013
DOI: 10.2478/bpasts-2013-0051

Modeling residual stresses generated in Ti coatings thermally sprayed on Al_2O_3 substrates

J. ZIMMERMAN[1], Z. LINDEMANN [1], D. GOLAŃSKI [2*],
T. CHMIELEWSKI [2], and W. WŁOSIŃSKI[3]

[1] Institute of Mechanics and Printing, Warsaw University of Technology, 85 Narbutta St., 02-524 Warsaw, Poland
[2] Institute of Manufacturing Processes, Department of Welding Engineering, Warsaw University of Technology, 85 Narbutta St., 02-524 Warsaw, Poland
[3] Institute of Fluid-Flow Machinery, Polish Academy of Sciences, 1 Defilad Sq., 00-901 Warszawa, Poland

Abstract. There is described a method of modeling by the finite element method the residual stresses induced during thermal deposition of coatings. The simulation was performed in two stages. The first dynamic stage simulated the impacts of the individual particles of the coating material onto the substrate, and the next static stage included a non-linear thermo-mechanical analysis intended for simulating the process of layer-by-layer deposition of the coating, with a specified thickness, and then cooling the entire system to the ambient temperature. In the computations, the samples were assumed to be cylindrical in shape and composed of an Al_2O_3 substrate and a titanium coating (with three different thicknesses) deposited using the detonation method. The correctness of the numerical model was verified experimentally by measuring the deflections of a real Ti coating/Al_2O_3 substrate sample with the Ti coating detonation-sprayed on the ceramic substrate, after cooling it to the ambient temperature. The experimental results appeared to be in good agreement with those obtained by the numerical computations.

Key words: residual stress, coatings, thermal spray.

1. Introduction

Thermal spraying methods are the most versatile techniques of depositing coatings on various substrates. They permit producing metallic, ceramic, and composite layers on metallic or ceramic substrates. In thermal spraying processes, hot or cold particles of the coating material are transported at a high velocity towards the substrate. When the particles impinge upon the substrate surface at a very high speed they undergo severe deformation and form the so-called lamella which 'anchor' themselves in the substrate thereby forming a multi-layer coating of a specified thickness [1–4]. In the final stage of the process the coated substrate is cooled to the ambient temperature. Because of the differences in their thermal, physical, and mechanical properties, the coating and substrate materials shrink in various degrees which results in residual stresses being induced during the cooling stage. The magnitude of the stresses is the higher the greater are the differences in the mechanical and thermal properties of the two materials (e.g. the mismatch between their thermal expansion coefficients), and the temperature differences between the substrate and the successive layers. The interface between coating and substrate, porosity of coating materials may also affect the temperature gradients that arise and influence the thermal stresses in bonded materials having different thermal properties [5–7].

Under cyclically varying loads, the residual stress state prevailing in the coating and the substrate affects essentially the mechanical strength, resistance to thermal shocks, and fatigue strength of the substrate-coating system [8–11]. The assessment of the magnitude of these stresses is therefore an important research problem.

The analysis of the residual stress state in thermally deposited coatings is conducted using analytical methods [12–14] which account for simplified coating/substrate models and by using numerical modeling supported by the finite element method [15–17]. The last approach allow to model complex geometries of coating/substrate systems as well as to conduct dynamic and static thermo-mechanical material modeling including plasticity effects [18–20]. Because the physical description of thermal spraying process is a very complex one the development of numerical model fully describing the deposition process and formation of residual stresses is a crucial task. The literature data contain several attempts to model the residual stress formation in thermally deposited coatings, but most of them still need some kind of model simplifications and analysis assumptions in order to built the discreet numerical model [1, 21–22].

The aim of this study was to construct a numerical model suitable for simulating the magnitude and distribution of the residual stresses induced during the thermal-deposition of coatings on a substrate. In particular, the model was designed for examining the residual stresses induced during depositing a titanium coating on an Al_2O_3 ceramic substrate using the detonation method. A titanium coating on Al_2O_3 substrate can serve as a metallization or intermediate layer that may allow direct bonding of alumina ceramics to other metals [23–24].

*e-mail: dgol@wip.pw.edu.pl

2. Assumption underlying modelling the residual stresses in thermally deposited coatings

The process of thermal-deposition of coatings has the two basic phases: dynamic impacts of the coating material particles onto the substrate or on the previously deposited layer, and the layer-by-layer formation of the coating on the substrate. Hence, the modeling of the residual stresses was also divided into two stages. The first dynamic stage included modeling the impacts of the individual particles on the substrate. The certain quantities obtained in the solution of the first-stage problem are taken as the boundary conditions in the next stage which included a coupled non-linear thermo-mechanical analysis of the formation of the subsequently growing sub-layers at prescribed time intervals (defined by the process parameters) until the coating acquires the prescribed thickness, and then cooling the entire coating-substrate system to the ambient temperature.

The processes of the thermal-deposition of coatings are complex and their course depends on many factors such as the condition and size of the coating particles, their impact velocity, the required final thickness of the coating, the kind of the bonded materials, the condition of the substrate surface, and the technique of cooling. Taking into account the complexity of the deposition process and the non-linear behaviour of the materials, we assumed certain simplifications of the physical process so that the numerical model used for the residual stress analysis in metallic and ceramic coatings could utilize the finite element method.

These assumptions were:

- The particles impinge onto the substrate which results in their deforming in a short time and considerable amount of their kinetic energy being transformed into thermal energy. In effect, the particles are flattened, form lamella which join to form thin plates (sub-layers). The next layers are successively deposited during each subsequent cycle thereby finally building the coating of the desired thickness.
- During a given cycle, all the particles impinging onto the substrate have the same initial temperature, and the individual layers formed of these particles during a single 'pass' are parallel to each other.
- The coating particles are in the softened state. Within the collision zone, the time taken for heating and cooling the particles is shorter than the duration of the spraying cycle by at least two orders of magnitude [25] so that the next particles are deposited on the preceding layer when it is already solidified. This assumption de-couples the problem to be simulated from the fluid dynamics approach and permits simplifying it to a thermo-mechanical problem [26]. The substrate and the previously deposited layers are modelled in the solid state with a prescribed temperature field, and their mechanical and physical properties are temperature-dependent.
- The effect of the phase transformations on the magnitude of the residual stresses is neglected [21].
- The substrate and the successive layers are in ideal contact.

3. Modeling the impacts of the particles onto the substrate

As shown in [3], no coagulation of the particles takes place during their movement to the substrate so that each particle may be considered individually i.e. as isolated from the other particles. Therefore, it is a single particle impinging on the substrate which is modeled. The distribution of the temperature established as a result of the transformation of the kinetic energy of the particle into deformation- and heat energies was computed using the ANSYS-AUTODYN program, and the analysis was considered to be dynamic of the 'explicit' type with the assumption of the ideal contact between the surfaces in touch and of the thermal-mechanical coupling between the phenomena involved. The heat transfer mechanism involves the heat conduction by the particle and the substrate. The computations were performed on the assumption that the process is adiabatic.

On the collision with the substrate, the particle or the substrate (depending on the kinds of the bonded materials) undergoes severe deformation at a high deformation rate. For metallic materials a plastic model was adopted, defined by Johnson-Cook [27], whereas the strength properties of ceramic materials were represented by the Johnson-Holmquist model [28].

The calculated temperature distribution was used for estimating the heat flux such that will give similar temperature distributions in the static model adopted at the second modeling stage. The course of deformation of the particle (initially spherical in shape) and of its acceleration along its path to the substrate were represented by a 3D (spatial) model. The deforming particles block each other thereby forming a uniform layer.

Modeling the dynamics of the particle movement was based on the simplifying assumption that all the particles have the same velocity perpendicular to the substrate and that they impinge on the substrate simultaneously forming a hexagonal configuration which ensures their maximum packing (Fig. 1a). The solution took into account the symmetry planes, which permitted the problem to be reduced. The blocking behaviour of the subsequent rows of particles was in the model ensured by locating adequately the contact planes. A schematic representation of the geometry of a fragment adopted in the computations, together with the displacement blocking planes is shown in Fig. 1b. The 3D model was constructed based on this geometry. The numerical calculations were performed with the FEM 'ADINA 8.6' software using a 'dynamic-explicit' analysis with explicit integration. The finite element model (FEM) is shown in Fig. 2 where the thickened mesh lines represent the contact planes.

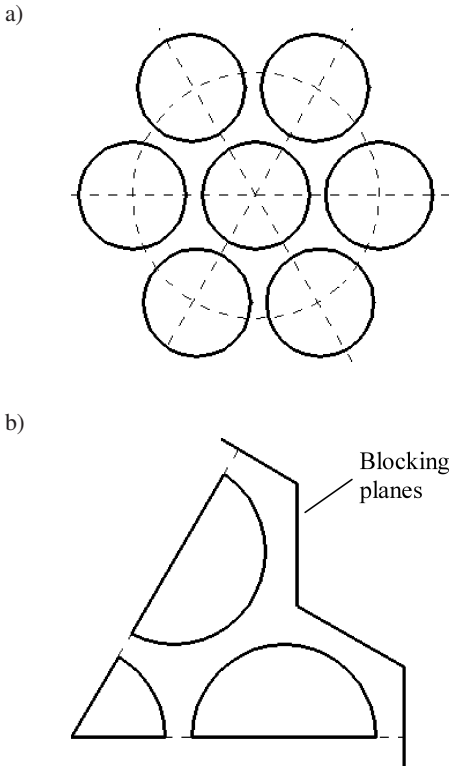

Fig. 1. Hexagonal arrangement of the spherical particles (a), schematic representation of the model geometry used in the calculations (b)

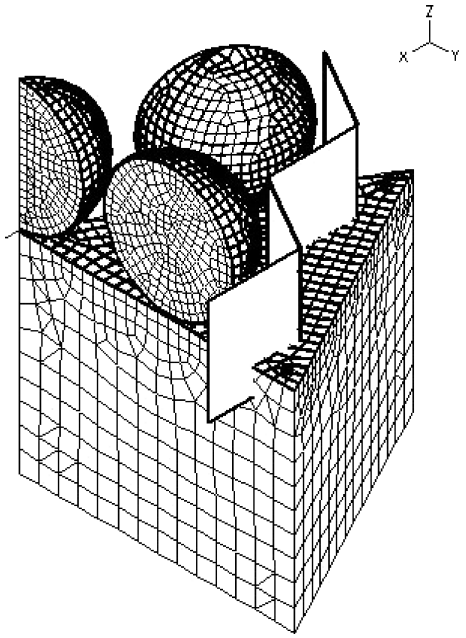

Fig. 2. Finite element model of Ti particles impacting into the Al_2O_3 substrate

4. Modeling the temperature field

Both components, the coating (denoted by index C) and the substrate (denoted by index S), were assumed to be cylindrical in shape, which simplified the problem to axisymmetric. The modeling process was divided into several stages with the calculations based on the equations of transient heat flow at each computation stage. The boundary and initial conditions were defined according to the assumptions:

- Stage 0 – the starting stage: the substrate material with prescribed physical properties (dependent on the temperature) is at room temperature. Within the prescribed short time interval t_0 the substrate is heated, beginning from its upper surface S_I, by the heat source which involves the ambience with the temperature T_z and heat exchange through the convection h_z resulted by the draught from the moving particles. The other surfaces of the substrate are at room temperature T_0 and heat transfer proceeds through free convection.
- Stage 1 – corresponds to the time t_I which elapses from the appearance of the first coating material sublayer with the prescribed properties and temperature T_{cI}, to the deposition of the next sub-layer. The interface surface between the substrate and the first coating sublayer is loaded with the heat flux q_I which acts for the very short time t_z. The heat flux was selected so that the temperature gradient in the substrate was the same as that calculated previously in the dynamic solution concerning the impact of a single particle into the substrate. The ambient temperature and convection conditions are the same as those adopted at the preceding modeling stage.
- Stage 2 – after the time $2t_I$ the next sublayer of the prescribed temperature T_{c2} appears. The interface between the first and the second sublayers is loaded with a heat flux q_2 active during time t_2. The ambient temperature and convection conditions remain the same as those in the preceding stage.
- Stage N – after the time Nt_I we have the n-th sublayer with the specified temperature T_{cN}. The boundary conditions are the same as in the preceding stages. The coating acquires the required thickness.
- Final stage – cooling the entire system to the ambient temperature T_0.

Figure 3 shows the up-dated geometry of the computation model and the initial and boundary conditions assumed in the analysis of heat transfer during the progressive growth of the coating. The solution of the temperature field problem was obtained using the thermal analysis module of the FEM ADINA 8.6 program. In the computations, 4-node axisymmetric conducting elements were used for the substrate and coating materials and 2-nodes convection elements at the edges. The conducting elements of the as-deposited sublayer and the convection elements of the upper and side surfaces of the coating are activated at the time intervals t_I, whereas at the same time the convection elements between the individual sublayers are disabled. Therefore, the modeling of the temperature field becomes a problem with variable boundary condition where the outer surface of the coating grows at a rate determined by the spraying technology employed.

sample radius r=13.5 mm; substrate thickness g_s=0.65 mm
total coating thickness g_c=0.1 mm (0.145 mm; 0.22 mm), coating sublayer thickness g_{c1}=0.05 mm
initial time of surface heating t_0=2 s; time between first and subsequent coating sublayers t_1=0.1 s
prescribed temperature of subsequent coating sublayers T_{c1}=90°C; T_{c2}=114°C ; T_{c3}=150°C
ambient temperatures T_0=25°C, T_z=150°C
convection at deposited surface h_z=100 W/m^{2}K; free convection h_0=10 W/m^{2}K
duration time of heat flux t_z=1 μs;
heat flux at the coating/substrate interface q_1=2600 W/m^2;
heat flux at subsequent coating sublayer interfaces q_2=1900 W/m^2

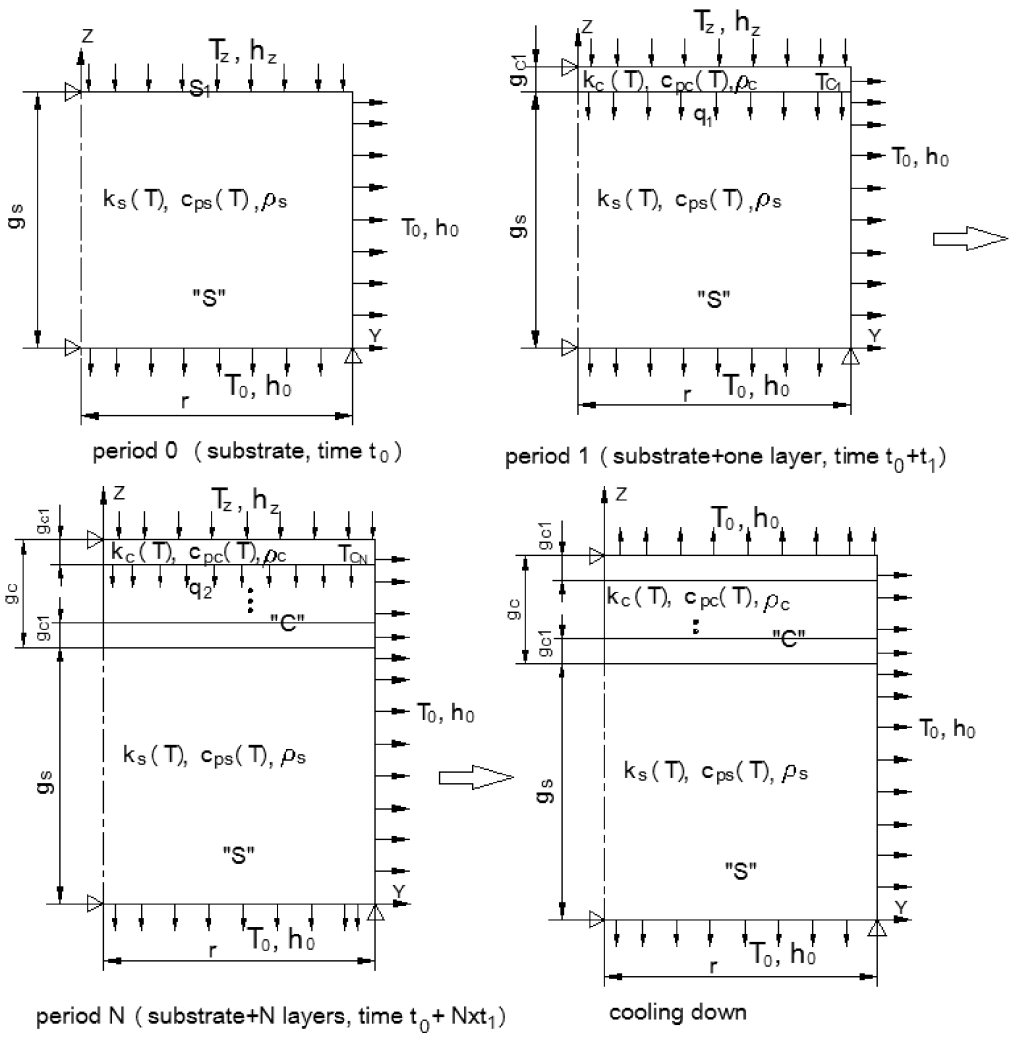

Fig. 3. Description of the initial and boundary conditions with updated model geometry assumed in the estimation of the temperature field in thermally deposited coatings

5. Modeling the stress field

The temperature field activates thermally the process of mechanical deformation. In the analysis of stresses, the load is therefore the temperature field known from the solution of the transient heat flow during the successive time increments with the newly-deposited sublayers being activated. During the series of time steps, the temperature field is superposed on the static mechanical field. The analysis was performed using the 'element birth' option of the FEM program. The static model also takes into account the effect of impacts of the individual coating particles on the substrate and on the just deposited sublayer. This was realized by making the load (active in a very short time of 1 μs) proportional to the mass and acceleration of each newly deposited sublayer. The particle acceleration was estimated from the course of the deformation vs time of the center of the coating material sphere, known from the solution of the dynamic problem concerning the impact of the particles on the substrate (ADINA program – explicite). The behavior of the ceramic substrate was assumed to be thermo-elastic, whereas that of the metallic materials – thermoplastic.

6. Computation results

6.1. Particle impacts onto the substrate and the preceding sublayer. Impact of a titanium particle onto the Al_2O_3 ceramic substrate was simulated using the ANSYS-AUTODYN program. The aim of the simulation was to determine the temperature field induced as a result of the kinetic energy of the particle being transformed into the energy of its plastic deformation and then its transformation into heat energy. It was assumed that 80% of the kinetic energy of impacting Ti particles is transformed into heat energy. The initial temperature of the Ti particle was assumed to be 300 K and its velocity to be 800 m/s. The assumption of low temperature of titanium particle was dictated by the fact that the substrate material is heated mainly by the energy coming from the particle impact. It was assumed that the particle is spherical in shape with the diameter d=0.050 mm and the substrate is sized at 0.4×0.65 mm.

Figure 4 shows a map of the temperature field after a time of 50 ns from the collision, and Fig. 5 shows the variation of the temperature vs. time at three characteristic points indicated in the figure (points A, B, and C). The temperature gradient estimated based on the temperature distribution was 22°C/μm. This increase of the temperature was taken into account in the next stage of the modeling of the coating deposition process, by selecting the heat flux (acting for $t_z = 1$ μs) so as to obtain the same temperature gradient.

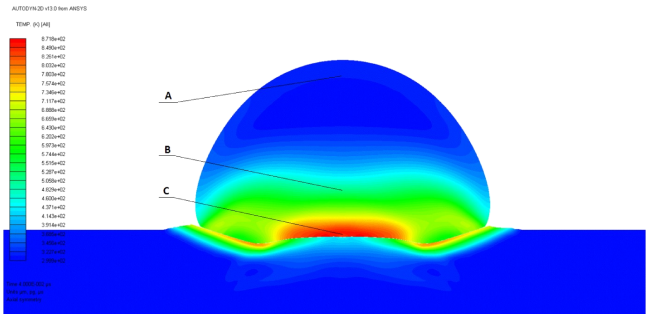

Fig. 4. Temperature distribution after 50 ns from the Ti impact into the Al_2O_3 substrate showing the measuring points

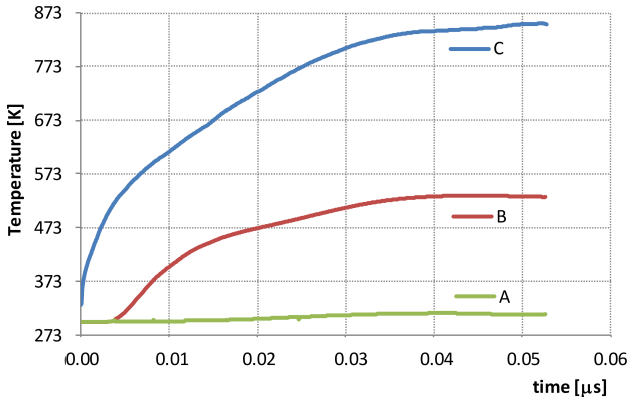

Fig. 5. Temperature distribution, due to the conversion of kinetic- into heat energy, determined at selected points of the Ti particle during its impact into the Al_2O_3 substrate

Two series of computations were then performed using the FEM ADINA 8.6 PROGRAM (dynamic-explicit). The first series included modeling the impacts of the Ti particles into the Al_2O_3 substrate, and the second – modeling the impacts of these particles in the previously deposited uniform Ti sublayer. The assumptions adopted in both series for titanium were: the initial particle velocity – 800 m/s, particle diameter $d = 50$ μm, specific weight $\gamma = 4.54$ g/cm^3, material model – elastic/plastic ('plastic bilinear'), Young modulus $E = 129040$ MPa, yield point R_e=500 MPa, and hardening module $E_u = 500$ MPa. The ceramic substrate was assumed to be an elastic material with the specific weight $\gamma = 3.9$ g/cm^3 and the elastic modulus $E = 318200$ MPa. The Ti particles were assumed to be in contact with one another, with the substrate and with the planes – which gives the total of 10 contacting pairs. Figure 6 shows deformation of the Ti particles after their impingement into the Al_2O_3 substrate as obtained in the first computation series. It can be seen that the particles have been flattened from both the side of the substrate and at their top surface. Moreover they have been brought in touch with one another so that they fill the free spaces between them. The ceramic substrate remains practically undeformed. Figures 7a and b show the vertical displacement and acceleration of the gravity center of the central spherical Ti particle. The visible oscillations of acceleration result from numerical differentiation procedures. Also, the detailed observation of the displacement curve allows to find inflection points. In effect the oscillations occur which are additionally exaggerated by the scale of acceleration axis.

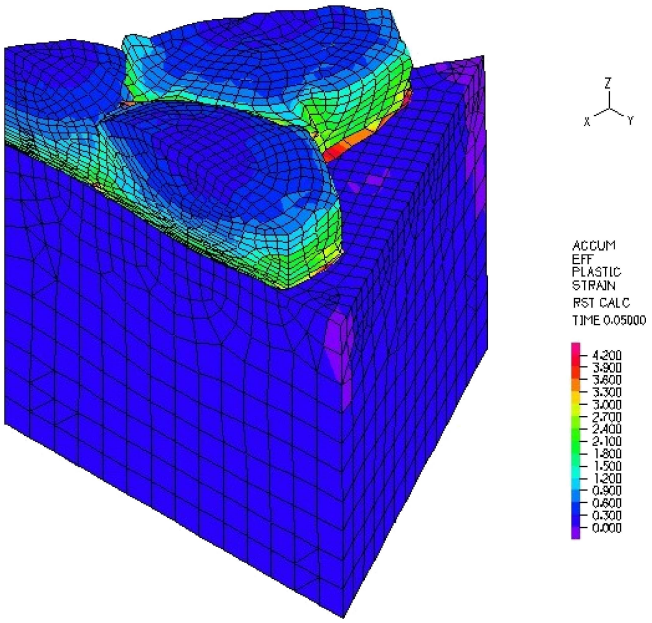

Fig. 6. Deformation and effective plastic strain distribution of the spherical Ti particles after their impact into the Al_2O_3 substrate

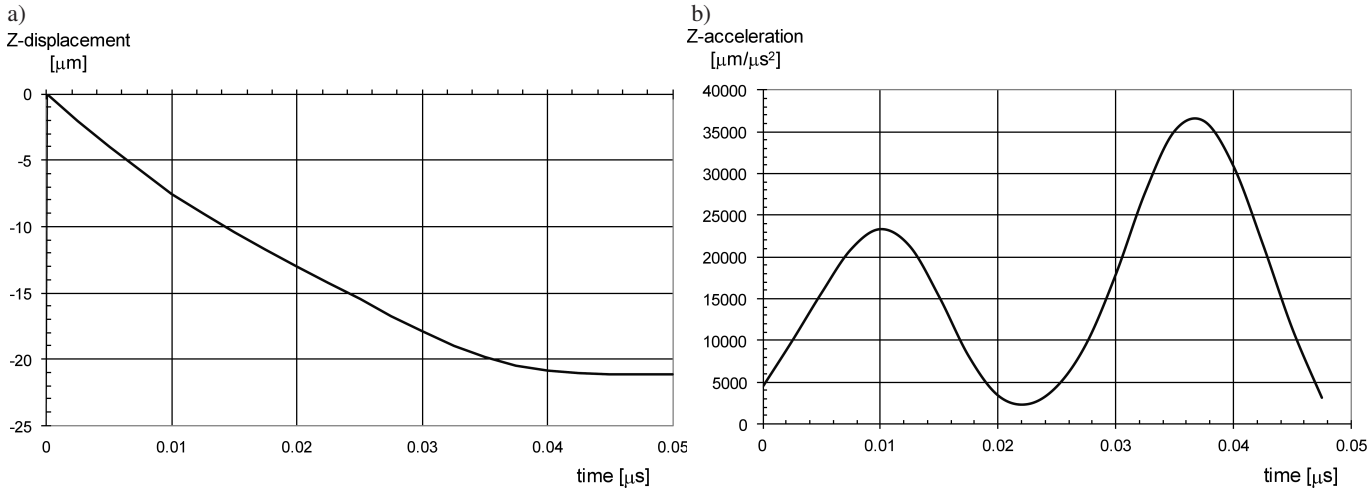

Fig. 7. Vertical displacement (a) and acceleration (b) of the center of gravity of the central Ti particle during its impact into Al_2O_3 substrate

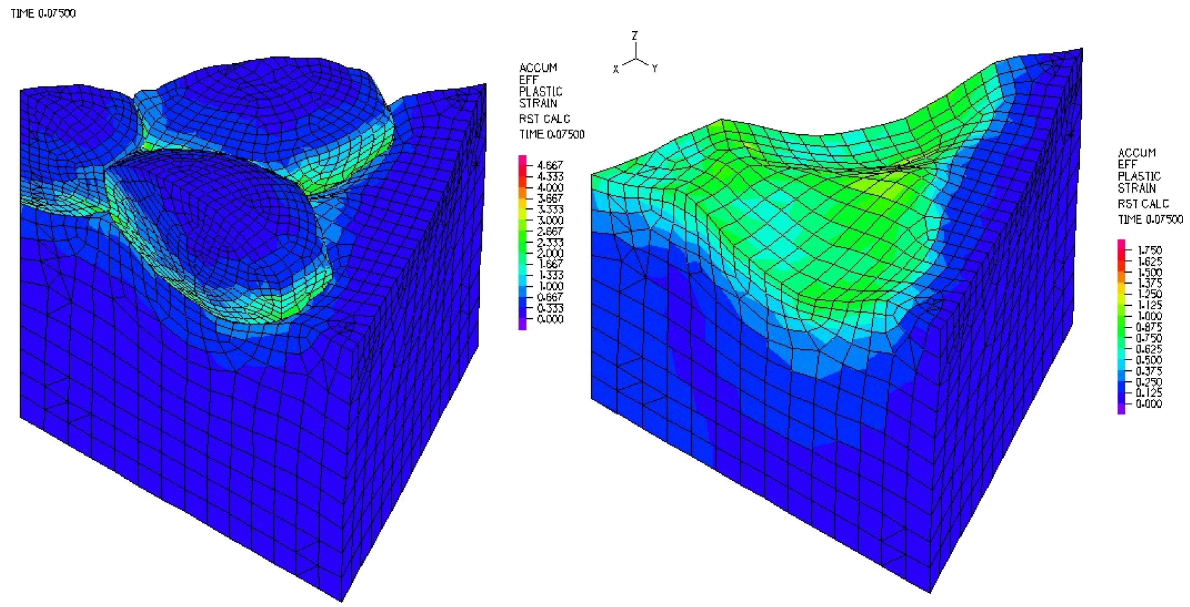

Fig. 8. Deformation and effective plastic strain distribution of spherical Ti particles after their impact into the previously deposited Ti sublayers

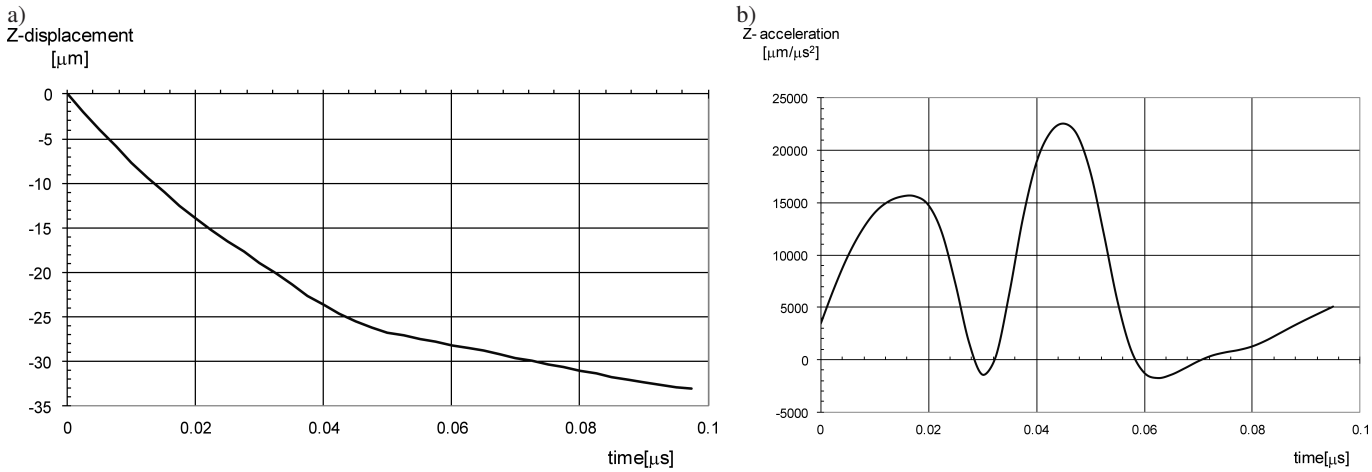

Fig. 9. Vertical displacement (a) and acceleration (b) of the center of gravity of the central Ti particle during its impact into the previously deposited Ti sublayers

The second computation series included modeling the impacts of the spherical Ti particles into the Ti substrate formed by the previously deposited sublayers (Fig. 8). It can be seen that in this case the impinging particles go dip into the preceding Ti sublayers. As in the first computation series, the deforming particles fill the free spaces between each other. Figures 9a and b show the vertical displacement and acceleration of the gravity center of the central spherical Ti particles.

6.2. Computed temperature distribution. The model was verified by measuring the deflection of the samples during the detonation-spraying of the Ti coating on the Al_2O_3 ceramic substrate. The samples were circular-symmetric in shape with a diameter of 27 mm, the substrate thickness was $g_s = 0.65$ mm, the substrate was covered with coatings of the 3 thicknesses $g = 0.1$ mm, 0.145 mm, and 0.2 mm. The thickness of the sublayer deposited in one shot was $g_1 = 0.05$ mm.

Tables 1 and 2 give the thermal, physical, and mechanical properties (time-dependent) of titanium and Al_2O_3 used in the numerical computations, based on the literature data [29, 30].

Figure 10 shows the calculated temperature distribution determined in the Ti coating-Al_2O_3 substrate system during the spraying process. The temperature profiles were drawn at the characteristic points on the sample axis. The coating was built of three sublayers and its total thickness was $g_c = 0.145$ mm.

We can see from Fig. 10 that the impact of the spherical Ti coating particles results in a violent increase, in a very short time (about 1 ms), of the temperature at the interfaces between the substrate and the sublayer and between the adjacent sublayers, after which the temperature of the entire system is quickly equalized until a new sublayer begins to grow. The ceramic substrate is heated up only slightly and, after the spraying cycle is completed, reaches a temperature of about 70°C.

Table 1
Physical and mechanical properties of Ti used in the calculations

T (K)	300	400	500	600	700	800	900	1000	1100	1200	1300
c_p (J/kgK)	523	546	561	597	632	672	700	729	685	637	658
λ (W/mK)	21.9	21.0	20.4	19.7	19.4	19.7	20.7	22.0	23.6	25.3	27.0
E (GPa)	129.8	128.8	126.8	123.8	120.0	115.0	109.0	103.0	95.5	87.2	78.0
R_e (MPa)	500	453	326	233	170	122	86	69	67	66	33
$\alpha \cdot 10^{-6}$ (1/K)	8.4	8.7	9.1	9.4	9.7	9.9	10.0	10.0	10.0	10.0	10.0

Table 2
Physical and mechanical properties of Al_2O_3 used in the calculations

T (K)	300	400	500	600	700	800	900	1000	1100	1200	1300
c_p (J/kgK)	754	951	1005	1089	1130	1151	1172	1214	1223	1235	1256
λ (W/mK)	34.6	25.1	19.0	14.7	11.2	9.5	8.6	6.9	6.0	5.1	5.0
E (GPa)	318.3	316.9	315.3	313.2	310.5	307.3	303.6	299.3	294.4	291.8	289.0
$\alpha \cdot 10^{-6}$ (1/K)	5.9	6.5	7.1	7.6	8.0	8.4	8.7	8.9	9.0	9.1	9.1

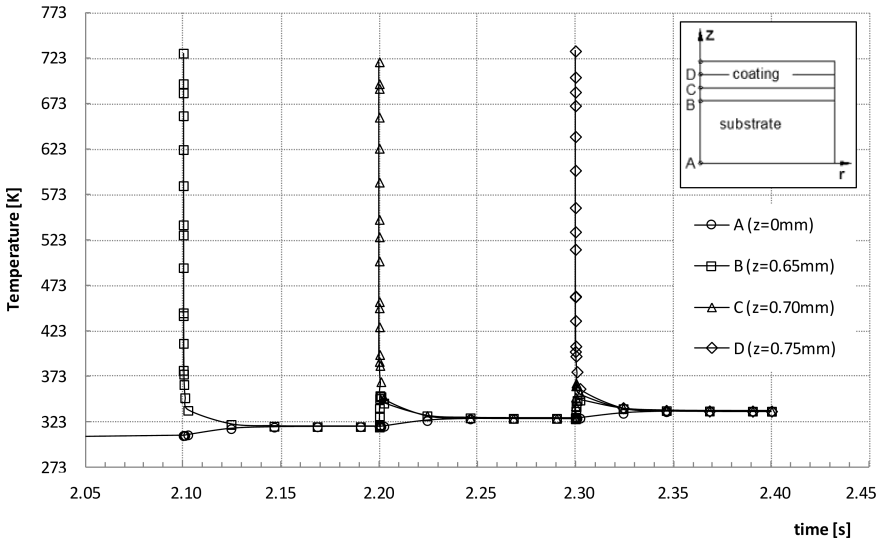

Fig. 10. History of the temperature distribution during thermal spraying, recorded at the characteristic points on the vertical axis of the Ti coating/Al_2O_3 substrate system

6.3. Distribution of residual stresses induced in the coating-substrate system and deflection of the system. Figures 11 and 12 show the results of computation of the distributions of the residual stresses induced in the Ti coating/Al_2O_3 system during the spraying process after cooling the system to room temperature. Figure 11 shows the maps of the radial and axial residual stresses. It can be seen that both the radial and axial stress distributions are uniform along the radius, except in the vicinity of the cylindrical side surface where the stresses are highly concentrated due to the singularity of the stress field at the edge of the system. Figure 12 shows the distribution of the radial residual stresses along the vertical axis of the sample (as a function of the distance from the coating/substrate interface) for three samples with differing coating thicknesses (0.1 mm, 0.145 mm and 0.22 mm). The diagrams indicate that within the regions near the point A (according to the notation in Fig. 10) the radial stresses in the substrate are tensile. In all the three samples, at the distance $g = 0.4$ mm down from the coating/substrate interface, the stresses become compressive. As the coating thickness increases the magnitude of the radial tensile stresses in this region increases up to 40 MPa. Within the narrow zone near the substrate/coating interface the radial stresses change their sign again to become tensile and reach a maximum of about 90 MPa in the sample with the coating thickness of 0.1 mm and 65 MPa in the sample with a 0.22 mm-thick coating.

In the thin transition layer at the coating/substrate interface near the coating the radial stresses are compressive in the samples with the thin coating whereas in the samples with the thicker coatings they become tensile and their magnitude is higher than that in the samples with the thinner coatings. The maximum tensile stress in the coating increases with increasing coating thickness and, in the sample with the thicker coating, slightly exceeds 200 MPa.

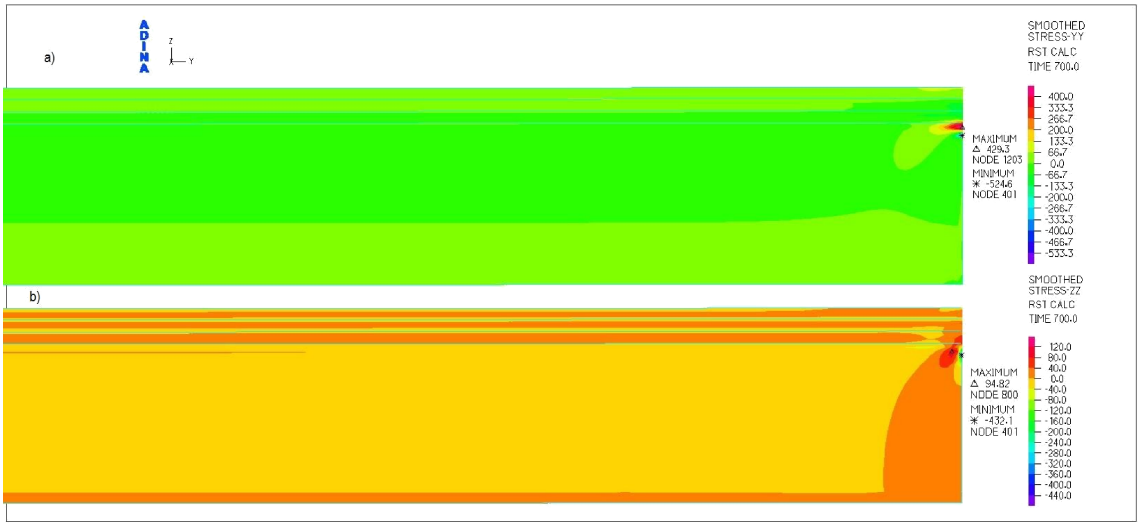

Fig. 11. Distribution of radial (a) and axial (b) residual stresses in the Ti-Al_2O_3 coating/substrate system

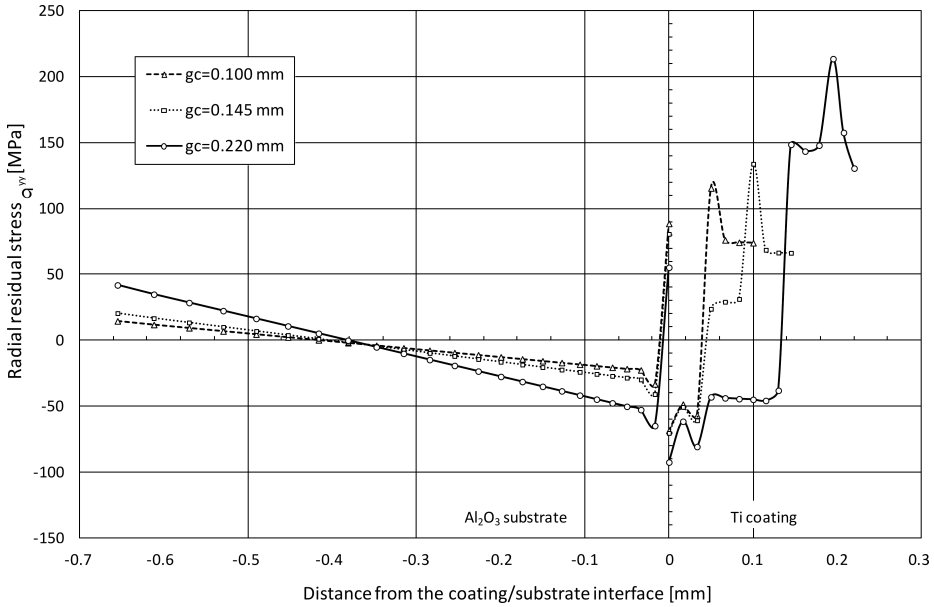

Fig. 12. Distribution of radial residual stresses along vertical axis (z=0) as a function of the distance from the Ti-Al_2O_3 interface, determined in three samples with various Ti coating thicknesses: 0.1 mm, 0.145 mm and 0.22 mm

The computation results were experimentally verified by measuring the deflections of the Ti/Al_2O_3 samples after the detonation spraying process. For this purpose we used the experimental valveless detonation gun. The barrel of the gun had 1000 mm length and 25 mm diameter. The mixture of propane and oxygen (propane pressure 0.08 MPa, oxygen pressure 0.12 MPa) was used as a detonation gas and nitrogen (pressure 0.08 MPa) as a purge gas. The distance between the end of the detonation barrel and the substrate material was kept at 160 mm. The coating was deposited in a discrete manner with frequency of detonation equal to 4 Hz. The coating material was pure titanium (99.7%) in the form of power with particle diameter between 40–50 μm. It was deposited onto Al_2O_3 substrate samples with 0.65 mm thickness and 27 mm diameter. Figure 13 presents the microstructure of deposited titanium coating. The obtained coatings are even, with good adhesion to the substrate material and low porosity.

The deflection of coating/substrate system was measured after each coating deposition using digital dial gauge fixed in a special stand. The measurement was conducted at the center of the sample from the substrate side. The indication of the dial gauge was calibrated to zero for each ceramic substrate before the coating deposition. Figure 14 shows the deflections of the Ti/Al_2O_3 system (for the three thicknesses of the coating) calculated by the finite element method and the values of the maximum deflection of the Ti/Al_2O_3 samples (Ti-coated by spraying) measured at their half-length (point A in Fig. 9). The calculated and measured results obtained for the samples with the 0.1 mm – and 0.145 mm coatings are in very good agreement and in good agreement in the sample with the thickest thickness.

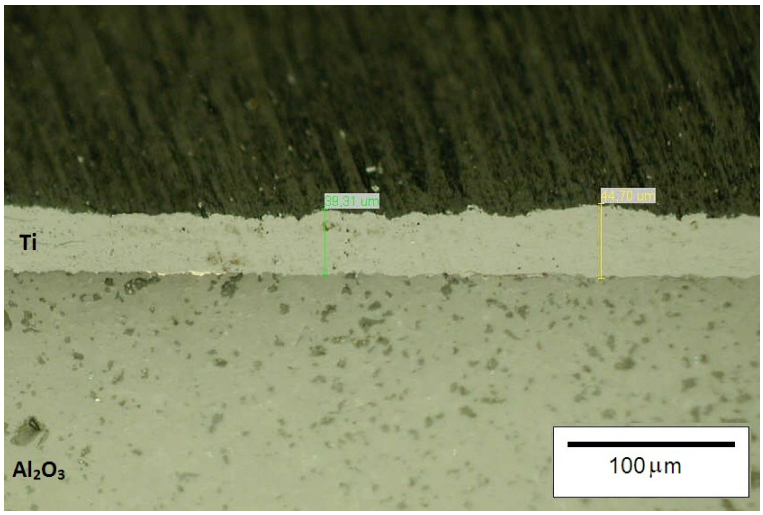

Fig. 13. The microstructure of titanium coating (~40 μm thickness) deposited onto Al_2O_3 substrate by the detonation gun method

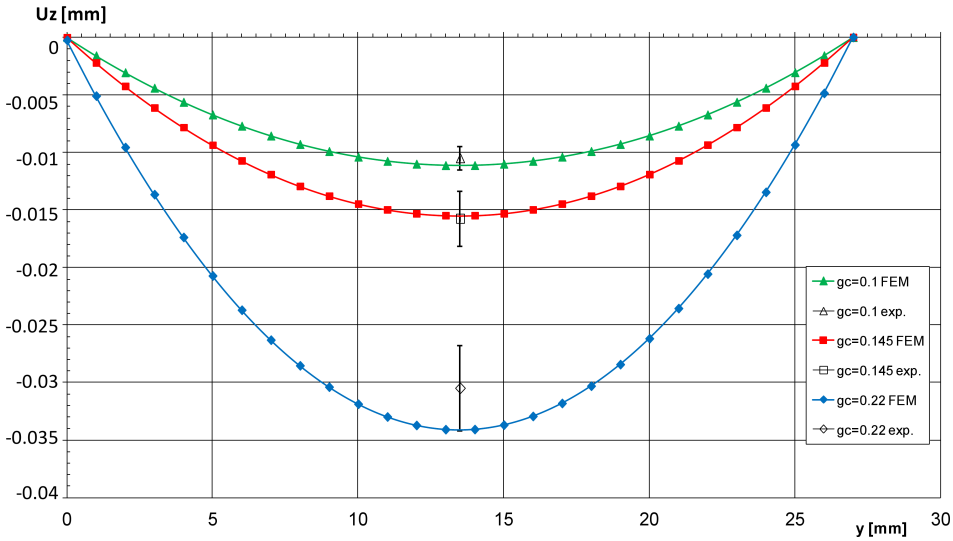

Fig. 14. Deflections of the Ti coating-Al_2O_3 substrate system calculated and measured for the three coating thicknesses

7. Conclusions

A numerical model based on the finite element method (FEM) was constructed for estimating the residual stresses induced in the coating/substrate system during thermal spraying of the coating on the substrate followed by cooling to room temperature. The modeling process was performed in two stages. The first dynamic stage included the simulation of the impacts of a single coating particle onto the substrate and onto the previously deposited coating sublayer. Some of the results obtained at this modeling stage were then utilized in the next static stage of the simulation process which consists of solving a thermo-mechanical problem concerning the layer-by-layer deposition of the coating during a certain time. The behavior of three Ti-coating/Al_2O_3 substrate systems with various coating thickness was simulated. The results of the FEM computations were compared with the results obtained experimentally. The conclusions are:

- the temperature gradient at the coating/substrate interfaces due to the particle impact energy was 22°C/μm,
- after its impact onto the Al_2O_3 substrate, the titanium particles were flattened by 56% (from 0.05 mm diameter to 0.022 mm height),
- on their impact into the ceramic substrate with a velocity of 800 m/s, the deceleration of the Ti particles due to their deforming in time is of the order of 38000 μm/s^2, whereas when the particles impinge on a Ti sublayer they are decelerated at 23000 μm/s^2,
- distributions of the radial and axial residual stresses in the coating/substrate system are uniform along the radius except at the outer cylindrical surface near the coating/substrate interface where they are highly concentrated,
- magnitude of the radial residual stresses in the Ti coating increases with its thickness, reaching a maximum of 200 MPa in the thickest coating,
- the numerical calculations of the maximum deflection of the Ti/Al_2O_3 model agree (within the tolerance limits) with their measured values obtained for the real samples. We can therefore conclude that the proposed numerical model well describes the process of formation of the coating and its deformation during the deposition process.

Further investigations should verify experimentally the assumptions adopted in the FEM computations, such as e.g., the prescribed temperature of the coating surface, convection coefficient, Young modulus E, yield point, and linear thermal expansion coefficient of the titanium coating.

Acknowledgements. This work has been supported by the National Science Center under the project No. N N519 652840.

REFERENCES

[1] Z. Gan and H.W. Ng, "Deposition-inducted residual stress in plasma-sprayed coatings", *Surface and Coating Technology* 187, 307–319 (2004).

[2] J. Stokes and L. Looney, "Residual stress in HVOF thermally sprayed thick deposits", *ICMCTF* 1, CD-ROM (2003).

[3] M. Li, P. Christofides, "Multi-scale modelling and analysis of an industrial hvof thermal spray process", *Chem. Eng. Sci.* 60, 3649–3669 (2005).

[4] N.J. Madejski, "Solidification of droplets on a cold surface", *Int. J. Heat Mass Transfer* 19, 1009–1013 (1976).

[5] M. Chmielewski and W. Weglewski, "Comparison of experimental and modelling results of thermal properties in Cu-AlN composite materials", *Bull. Pol. Ac.: Tech.* 61 (2), 507–514 (2013).

[6] K. Dems and Z. Mróz, "Analysis and design of thermo-mechanical interfaces", *Bull. Pol. Ac.: Tech.*, 60 (2), 205–213 (2012).

[7] K. Pietrzak, D. Kaliński, and M. Chmielewski, "Interlayer of Al_2O_3-Cr functionally graded material for reduction of thermal stresses in alumina – heat resisting steel joints", *J. Eur. Ceramic Society* 27 (2–3), 1281–1286 (2007).

[8] W.G. Mao and Y.C. Zhou, "Failure of thermal barrier ceramic coating induced by buckling due to temperature gradient and creep", *Advanced Materials Research* 9, 31–40 (2005).

[9] W. Wlosinski and T. Chmielewski, "Plasma-hardfaced chromium protective coatings-effect of ceramic reinforcement on their wettability by glass", *Proc. 3rd Int. Conf. Surface Engineering* 1, 48–53 (2002).

[10] A.N. Khan, J. Lu, and H. Liao, "Effect of residual stresses on air plasma sprayed thermal barrier coatings", *Surface and Coatings Technology* 168, 291–299 (2003).

[11] W. Węglewski, M. Basista, M. Chmielewski, and K. Pietrzak, "Modelling of thermally induced damage in the processing of Cr-Al_2O_3 composites", *Composites Part* B 43 (2), 255–264 (2012).

[12] Y.C. Tsui and T.W. Clyne, "An analytical model for predicting residual stresses in progressively deposited coatings. Part 1: Planar geometry", *Thin Solid Films* 306, 23-33 (1997).

[13] A. Mezin, "Coating internal stress measurement through the curvature method: A geometry-based criterion delimiting the relevance of Stoney's formula", *Surface and Coatings Technology* 200, 5259–5267 (2006).

[14] X. Feng, Y. Huang, and A.J. Rosakis, "On the Stoney formula for a thin film/substrate system with nonuniform substrate thickness", *Trans. ASME* 74, 1276–1281 (2007).

[15] D. Golański, T. Wierzchoń, and P. Biliński, "Numerical modelling of the residual stresses in borided layers on steel substrate", *J. Materials Science Letters* 14, 1499–1501 (1995).

[16] M. Toparlia, F. Sen, O. Culha, and E. Celik, "Thermal stress analysis of HVOF sprayed WC–Co/NiAl multilayer coatings on stainless steel substrate using ?nite element methods", *J. Materials Processing Technology* 190, 26–32 (2007).

[17] T. Chmielewski and D. Golański, "Selected properties of Ti coatings deposited on ceramic AlN substrates by thermal spraying", *Welding Int.* 1, 1–6 (2011).

[18] X.C. Zhang, B.S. Xu, H.D. Wang, and Y.X. Wu, "Modeling of the residual stresses in plasma-spraying functionally graded ZrO_2/NiCoCrAlY coatings using ?nite element method", *Materials and Design* 27, 308–315 (2006).

[19] P. Bengtsson and C. Persson, "Modelled and measured residual stresses in plasma sprayed thermal barrier coatings", *Surface and Coatings Technology* 92, 78–86 (1997).

[20] R. Ghafouri-Azar, J. Mostaghimi, and S. Chandra, "Modeling development of residual stresses in thermal spray coatings", *Computational Material Science* 35, 13–26 (2006).

[21] X. Zhang, J. Gong, and S. Tu, "Effect of spraying condition and material properties on the residual stress in plasma

spraying", *J. Material Science Technology* 20 (2), 149–153 (2004).

[22] S. Widjaja, A.M. Limarga, and T.H. Yip, "Modeling of residual stresses in a plasma-sprayed zirconia/alumina functionally graded-thermal barrier coating", *Thin Solid Films* 434, 216–227 (2003).

[23] K.-R. Donner, F. Gaertner, and T. Klassen, "Metallization of thin Al_2O_3 layers in power electronics using cold gas spraying", *J. Thermal Spray Technology* 20 (1–2), 299–306 (2011).

[24] T. Chmielewski, "Application of kinetic energy of friction and detonation wave for metallisation of ceramics", *Scientific Papers of Warsaw University of Technology. Mechanic Series* 242, 1–157 (2012), (in Polish).

[25] T. Watanabe, I. Kuribayashi, T. Honda, and A. Kanzawa, "Deformation and solidification of a droplet on a cold substrate", *Chem. Eng. Sci.* 47, 3059–3065 (1992).

[26] C.H. Amon, R. Merz, F.B. Prinz, and K.S. Schmaltz, "Numerical and experimental investigation of interface bonding via substrate melting of an impinging molten metal droplet", *J. Heat Transfer* 118, 16-172 (1996).

[27] G.R. Johnson and W.H. Cook, "A constitutive model and data for metals subjected to large strains, high strain rates, and high temperatures", *Proc. 7th Int. Symp. on 'Ballistics'* 1, 541–547 (1983).

[28] G.R. Johnson and T.J. Holmquist, "An improved computational constitutive model for brittle materials", *High-Pressure Science and Technology* 309, 981–984 (1994).

[29] R. Boyer, G. Welsch, and E. Collings, *Materials Property Handbook: Titanium Alloys*, ASM International, Materials Park, 1994.

[30] A. Goldsmith, T.E. Waterman, and H.J. Hirchorn, "*Handbook of Thermophysical Properties of Solid Materials*", Academic Press, New York, 1961.